Available online at www.sciencedirect.com
ScienceDirect
Journal of Sound and Vibration 310 (2008) 587–607
JOURNAL OF SOUND AND VIBRATION
www.elsevier.com/locate/jsvi

# The effect of critically moving loads on the vibrations of soft soils and isolated railway tracks

L. Auersch*

*Federal Institute for Materials Research and Testing, D 12200 Berlin, Germany*

Accepted 2 October 2007
The peer review of this article was organized by the Guest Editor
Available online 26 November 2007

**Abstract**

The dynamic response of the railway track is strongly influenced by the underlying soil. For a soft soil and very high train speeds or for a very soft soil and regular train speeds, the train speed can be close to the speed of elastic waves in the soil. This paper presents a detailed study of the so-called "moving-load effect", i.e. an amplification of the dynamic response due to the load movement, for the tracks on soft soil. The analysis is carried out by evaluating the related integrals in the wavenumber domain. The influence of the load speed is quantified for a large set of parameters, showing that the effect on the soil vibration is reduced with increase of the frequency, track width and inverse wave velocity. Therefore, the moving-load effect associated with vibratory train loads is negligible whereas the amplification associated with the moving dead weight of the train can be significant. The strong moving-load effect on a perfectly homogeneous soil, however, can be strongly diminished by a layered or randomly varying soil situation. This theoretical result is affirmed by measurements at a test site in Germany where the trains run on a very soft soil at a near-critical speed. The results for soft soils are compared with experimental and theoretical results for a stiff soil. It is found that the influence of the stiffness of the soil is much stronger than the moving-load effect. This holds for the soil vibration as well as for the track vibration which both show a minor dependence on the load speed but a considerable dependence on the soil stiffness in theory and experiment.

Railway tracks can include soft isolation elements such as rail pads, sleeper shoes and ballast mats. For these types of isolation elements and normal soil conditions, the influence of the load speed is usually negligible. There is only one isolation measure for which the moving load may be effective: a track which is constructed as a heavy mass–spring system. The resonance of this track system is shifted to lower frequencies and amplitudes for increasing train speed. A critical train speed can be reached if the mass–spring system has a marginal bending stiffness along the track.


## 1. Introduction

When running on imperfect wheels and imperfect tracks, trains generate dynamic vibratory loads on the railway tracks, which cause vibrations of the track and the surrounding soil. These ground vibrations caused by irregularities of the vehicle and track and the corresponding dynamic loads have been investigated recently

*Tel.: +49 30 8104 3290; fax: +49 30 8104 1727.
*E-mail address:* lutz.auersch-saworski@bam.de

0022-460X/$ - see front matter © 2007 Elsevier Ltd. All rights reserved.
doi:10.1016/j.jsv.2007.10.013

in Refs. [1,2], where it has been stated that the dynamic loads are the main cause of the ground vibration. During the last decade, there was a great scientific interest to the dynamic effects associated with train–track interaction [3–10]. The research was motivated by the growing high-speed traffic and the existence of soft soils for which the train speed could be as high as the wave speed of the soil. In Ref. [11], it was shown for moving loads of constant magnitude (hereafter, these loads are called static), that in most cases the regular response to the static load is quasi-static and no special moving-load effect occurs. This regular (quasi-static) response has only remarkable amplitudes at very low frequencies and at very short distances from the track. Therefore, the static loads can be regarded as a minor source of ground vibration for *normal* traffic and soil conditions. The present contribution examines the *special* conditions under which moving-load effect can be of importance in reality.

First, moving-load effects have been studied for beam structures and beams on Winkler foundation [12,13]. A number of newer studies use the elastic half-space as the model of the soil [14–18]. The effect of the moving load can be included in the computation by using stationary load spectra of the train [14,16] or by time simulation [17]. The present contribution uses the same basic formulas in the frequency–wavenumber domain as those presented in Refs. [3–10]. The wavenumber integral can be solved by the double fast Fourier transform algorithm [6,8], which yields a detailed wave field and corresponding surface and contour plots (Fig. 1). Other methods are more focused on the most important part of the transfer function for example by using the wavelet transform [5], analytical integration [4], or adjusted integration schemes [9, present contribution]. Up to now, two-dimensional wave-fields have been presented as examples for the capabilities of the method [5,6,8], and some more detailed results have been presented in Refs. [6–9] for the comparison with the Ledsgard measurements in Sweden [19,20]. In the present contribution, the double infinite wavenumber integral is evaluated for several cases and parameters to find the rules for the moving-load effects.

The critical train speed is, in practice, only reached on very soft soils. Therefore, the influence of the critical train speed is always combined with the influence of the reduced soil stiffness. Very soft soils yield completely different track behaviour and ground-borne vibration compared to normally stiff soils. In the present contribution, the results of a very soft soil are compared with the results of a normally stiff soil, and this comparison is also done for two corresponding soft and stiff measuring sites.

The contribution consists of three parts. Section 2 briefly describes the methods of calculation. In Section 2.1 the methods are discussed for the wave propagation of the soil, whereas in Section 2.2 the methods are shown for the combined track–soil system. Section 3 presents some results regarding the wave propagation through the soil. The effect of a moving load is studied for harmonic loads and constant loads separately. The case of moving harmonic loads with minor amplifications is treated in the first subsection whereas the case of a moving constant load with major effects is analysed in more detail in the second subsection. At the end of this section, the theoretical results are compared with measurements of a stiff and soft soil. The third main part (Section 4) analyses the track behaviour under moving loads. In Section 4.1, the influence of the homogeneous and layered

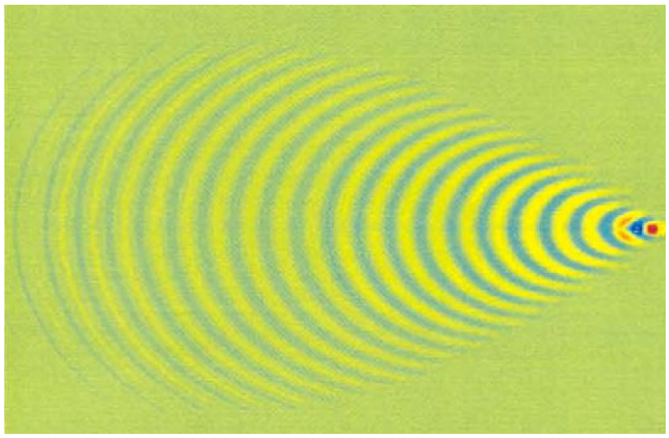

Fig. 1. Wave-field generated by a super-critically moving harmonic load, contour plot from the two-dimensional FFT method.

soil is established and compared with experimental results. A second subsection considers a track which is constructed as a heavy mass–spring system.

## 2. Methods of calculation

### 2.1. Wave propagation in the frequency–wavenumber domain

Consider a complex vertical harmonic load

$$p(x,y,t) = P\,\mathrm{e}^{\mathrm{i}\Omega t} p_1(x) p_2(y-vt) \tag{1}$$

with frequency $\Omega$ that moves in $y$-direction along the surface of a half-space. The vertical ground vibration at a distance $x$ from the track has to be calculated. The solution is found by transforming the stress field $p$ into the frequency–wavenumber domain, multiplying the load $p^*$ by the transfer function $H^*$ of the soil and calculating the inverse transform of the result into the $x$–$y$-plane. These three steps are performed as follows.

The excitation force is transformed into the frequency–wavenumber domain as

$$\begin{aligned}
p^*(k_x,k_y,\omega) &= \int_{-\infty}^{+\infty}\int_{-\infty}^{+\infty}\int_{-\infty}^{+\infty} p(x,y,t)\mathrm{e}^{-\mathrm{i}(k_x x+k_y y+\omega t)}\,\mathrm{d}x\,\mathrm{d}y\,\mathrm{d}t \\
&= \int_{-\infty}^{+\infty}\int_{-\infty}^{+\infty}\int_{-\infty}^{+\infty} P\,\mathrm{e}^{\mathrm{i}\Omega t} p_1(x) p_2(y-vt)\mathrm{e}^{-\mathrm{i}(k_x x+k_y y+\omega t)}\,\mathrm{d}x\,\mathrm{d}y\,\mathrm{d}t \\
&= P\int_{-\infty}^{+\infty} \mathrm{e}^{\mathrm{i}(\Omega-\omega)t}\int_{-\infty}^{+\infty} p_2(y-vt)\,\mathrm{e}^{-\mathrm{i}k_y y}\,\mathrm{d}y\,\mathrm{d}t\int_{-\infty}^{+\infty} p_1(x)\mathrm{e}^{-\mathrm{i}k_x x}\,\mathrm{d}x \\
&= P\int_{-\infty}^{+\infty} \mathrm{e}^{\mathrm{i}(\Omega-\omega)t} p_2^*(k_y)\mathrm{e}^{-\mathrm{i}k_y vt}\,\mathrm{d}t p_1^*(k_x) \\
&= P\int_{-\infty}^{+\infty} \mathrm{e}^{\mathrm{i}(\Omega-k_y v-\omega)t}\,\mathrm{d}t p_1^*(k_x) p_2^*(k_y) \\
&= P2\pi\delta(\omega-\Omega+k_y v) p_1^*(k_x) p_2^*(k_y).
\end{aligned} \tag{2}$$

In this contribution, only constant square loads of length $a$ are used as excitation

$$p_1(x) = \begin{cases} 1/a & \text{for } |x|<a/2, \\ 0 & \text{else,} \end{cases} \tag{3}$$

and the wavenumber transforms $p_1^* = p_2^*$ can be given explicitly as

$$p_1^*(k_x) = \frac{\sin k_x a/2}{k_x a/2}, \quad p_2^*(k_y) = \frac{\sin k_y a/2}{k_y a/2}. \tag{4}$$

The vertical compliance $u^*/p^* = H^*(\omega,k)$ of the soil for a vertical harmonic planar stress wave of circular frequency $\omega$ and wavenumber $k$ is calculated according to Ref. [21] or Ref. [22]. The homogeneous half-space is described by the shear modulus $G$, the shear and compressional wave velocities $v_S$ and $v_P$, and the compliance can be given explicitly as

$$H^* = \frac{q_P k_S^2}{\mathrm{i}G\det K} \tag{5}$$

with

$$\det K = (k_S^2 - 2k^2)^2 + 4k^2 q_S q_P \tag{6}$$

and

$$\begin{aligned}
k_S &= \omega/v_S, \quad q_S = \sqrt{k_S^2 - k^2}, \\
k_P &= \omega/v_P, \quad q_P = \sqrt{k_P^2 - k^2}.
\end{aligned} \tag{7}$$

The transfer function $H^*$ of the homogeneous or layered soil is used to establish the solution

$$u^*(k_x,k_y,\omega)=H^*(k_x,k_y,\omega)p^*(k_x,k_y,\omega) \tag{8}$$

in the frequency–wavenumber domain. The solution in the space domain is found by the inverse Fourier transform

$$\begin{aligned}u(x,y,t)&=\frac{1}{(2\pi)^3}\int_{-\infty}^{+\infty}\int_{-\infty}^{+\infty}\int_{-\infty}^{+\infty}H^*(k_x,k_y,\omega)P2\pi\delta(\omega-\Omega+k_yv)p_1^*(k_x)p_2^*(k_y)\mathrm{e}^{\mathrm{i}(k_xx+k_yy+\omega t)}\,\mathrm{d}k_x\,\mathrm{d}k_y\,\mathrm{d}\omega\\&=\frac{P}{(2\pi)^2}\int_{-\infty}^{+\infty}\int_{-\infty}^{+\infty}H^*(k_x,k_y,\Omega-k_yv)p_1^*(k_x)p_2^*(k_y)\mathrm{e}^{\mathrm{i}(k_xx+k_yy-k_yvt+\Omega t)}\,\mathrm{d}k_x\,\mathrm{d}k_y.\end{aligned} \tag{9}$$

If a moving coordinate system with

$$y^*=y-vt \tag{10}$$

is used, the integral is constant in time and the response of the soil to the moving load can be expressed as

$$u(x,y^*,\Omega)=\frac{P}{(2\pi)^2}\int_{-\infty}^{+\infty}\int_{-\infty}^{+\infty}H^*(k_x,k_y,\Omega-k_yv)p_1^*(k_x)p_2^*(k_y)\mathrm{e}^{\mathrm{i}(k_xx+k_yy^*)}\,\mathrm{d}k_x\,\mathrm{d}k_y \tag{11}$$

in the moving frame of reference. This resulting double integral is the same integral that has to be solved for a stationary load. The only difference between a moving and a stationary load is that the compliance of the soil has to be calculated for shifted frequencies

$$\omega=\Omega-k_yv \tag{12}$$

in case of the moving load.

### 2.2. Track deformation and track–soil interaction in the frequency–wavenumber domain

If the soil is loaded indirectly via the track system, the compliance of the combined track–soil system must be calculated. The most simple track system consisting of a track beam is considered as an example. A constant vertical stress is assumed across the width $a$ of the track, and the vertical compliance of the track–soil system is calculated at the centre line of the track. Other stress distributions and the approximation of a rigid behaviour of the track cross section can be considered, see Ref. [23] for details.

The problem is solved in the $k_y$–$\omega$-domain. The compliance $H_S$ of the soil for a harmonic wave strip load is calculated as

$$H_S(k_y,\omega)=\frac{1}{2\pi}\int_{-\infty}^{+\infty}H^*(k_x,k_y,\omega)p_1^*(k_x)\mathrm{d}k_x=\frac{1}{K_S(k_y,\omega)}. \tag{13}$$

The integral represents the displacement of the beam centreline for a constant stress distribution $p_1(x)$ across the track beam. The stiffness $K_S$ of the soil is combined with the stiffness $K_B$ of the beam

$$K_B(k_y,\omega)=EIk_y^4-m'\omega^2 \tag{14}$$

with bending stiffness $EI$ and mass density $m'$, to obtain the stiffness of the coupled beam–soil system

$$\begin{aligned}K_{BS}(k_y,\omega)&=K_B+K_S,\\H_{BS}(k_y,\omega)&=\frac{1}{K_B+K_S}.\end{aligned} \tag{15}$$

The force on the ground is calculated by the transfer function

$$T_{BS}(k_y,\omega)=\frac{K_S}{K_B+K_S}, \tag{16}$$

which relates the forces under the beam to the forces on the beam.

The displacements of the track are found by the inverse Fourier transformation of the displacements $u^*$ in the frequency–wavenumber domain

$$u^*(k_y,\omega) = H_{BS}(k_y,\omega)P,$$
$$u(y,\omega) = \frac{P}{2\pi}\int_{-\infty}^{+\infty} H_{BS}(k_y,\omega)\mathrm{e}^{\mathrm{i}k_y y}\,\mathrm{d}k_y \tag{17}$$

for a point load on the beam which has the constant wavenumber transform $P$. The displacements $u_S$ of the soil are calculated from the soil stresses under the beam

$$p_S^*(k_x,k_y,\omega) = T_{BS}(k_y,\omega)Pp_1^*(k_x) \tag{18}$$

with the representation (8) of the last section and the inverse Fourier transformation

$$u_S(x,y,\omega) = \frac{P}{(2\pi)^2}\int_{-\infty}^{+\infty}\int_{-\infty}^{+\infty} H^*(k_x,k_y,\omega)T_{BS}(k_y,\omega)p_1^*(k_x)\mathrm{e}^{\mathrm{i}(k_x x+k_y y)}\,\mathrm{d}k_x\,\mathrm{d}k_y. \tag{19}$$

Once again, the moving-load solution is established by the substitution of $\Omega - k_y v$ for $\omega$ and $y^* = y - vt$ for $y$ as

$$u_S(x,y^*,\Omega) = \frac{P}{(2\pi)^2}\int_{-\infty}^{+\infty}\int_{-\infty}^{+\infty} H^*(k_x,k_y,\Omega-k_y v)T_{BS}(k_y,\Omega-k_y v)p_1^*(k_x)\mathrm{e}^{\mathrm{i}(k_x x+k_y y^*)}\mathrm{d}k_x\,\mathrm{d}k_y \tag{20}$$

for the soil and

$$u_T(y^*,\Omega) = \frac{P}{2\pi}\int_{-\infty}^{+\infty} H_{BS}(k_y,\Omega-k_y v)\mathrm{e}^{\mathrm{i}k_y y^*}\,\mathrm{d}k_y \tag{21}$$

for the centre line of the track.

All integrals (11), (20) and (21) are solved numerically. The integration steps in the wavenumber domain are fitted to the compliance $H^*$ of the soil so that the important contributions of the poles of the compliance function are well incorporated. Special care is necessary for the static case $\omega = 0$, where all poles are at $k = 0$. The realistic material damping $D$ of the soil, which is introduced as $G = G_0(1+\mathrm{i}2D)$, facilitates the numerical integration.

## 3. Soil vibrations due to moving constant and harmonic loads

### 3.1. The influence of moving harmonic loads on soils with different stiffnesses

At first, the vertical transfer functions due to vertical stationary point loads are considered for three different homogeneous soils with $v_S = 300$, 100 and 30 m/s. A rather high damping value $D = 5\%$ is used in the calculations which has been determined experimentally at the measuring sites (see Section 3.3 and Table 1). The transfer functions of the soil particle velocities (Fig. 2, $v_S = 300$ m/s) show generally an increasing behaviour with frequencies increasing from 4 to 100 Hz which is the relevant frequency range for railway induced ground vibrations. For a soft soil with $v_S = 100$ m/s, the material damping causes a strong reduction of the amplitudes at high frequencies and far distances (Fig. 3). At low frequencies, the amplitudes are 10 times higher compared to the stiff soil. This effect is even stronger for the very soft soil of $v_S = 30$ m/s (Fig. 4). The low-frequency amplitudes of the soft soil are 100 times higher than the amplitudes of the stiff soil corresponding to the inverse ratio of the shear moduli. Due to the strong effect of damping for soft soils, the amplitudes are decreasing with higher frequencies in clear contrast to the transfer functions of the stiff soil.

Next, moving harmonic loads are considered. It is assumed that the load is uniformly distributed over a square area of width $a$ for which the values $a = 1.0$ and 2.6 m have been chosen. The moving-load effect for different load frequencies and wave velocities of the soil is derived by the following procedure which is illustrated by Figs. 5 and 6. For certain distances $x = 4$, 8, 16 m from the track, the displacements on a line parallel to the track are calculated. Fig. 5 shows an example for a small load area ($a = 1.0$ m), a medium stiff soil ($v_S = 200$ m/s) and a frequency of 8 Hz. For the critical speed, the amplitudes are much more concentrated and have a considerably increased maximum compared to the displacement $u_0(y)$ of the

Table 1
Parameters of the different soils

| $h$ | $v_S$ | $v_P$ | $G$ (MN/m) | $D = D_S = D_P$ | Figures |
|---|---|---|---|---|---|
| Stiff soil | | | | | |
| Homogeneous | 300 | 600 | 180 | 5 | 2, 18 |
| Medium soil | | | | | |
| Homogeneous | 200 | 400 | 80 | 5 | 5, 7, 8 |
| Soft soil | | | | | |
| Homogeneous | 100 | 200 | 20 | 5 | 3, 7, 8 |
| Very soft soil | | | | | |
| Homogeneous | 30 | 60 | 1.8 | 5 | 4, 6, 9, 10, 11, 19 |
| Layered soil | | | | | |
| 0–3 m | 30 | 60 | 1.8 | 5 | 11, 20 |
| >3 m | 300 | 600 | 180 | 5 | |
| Stiff site | | | | | |
| 0–5 m | 270 | 540 | 146 | 5 | 12, 15, 17a |
| >5 m | 1000 | 2000 | 2000 | 5 | 21, 23 |
| Very soft site | | | | | |
| 0–3 m | 30 | 60 | 1.8 | 5 | 13, 14, 16, 17b |
| >3 m | 300 | 600 | 180 | 5 | 22, 24 |

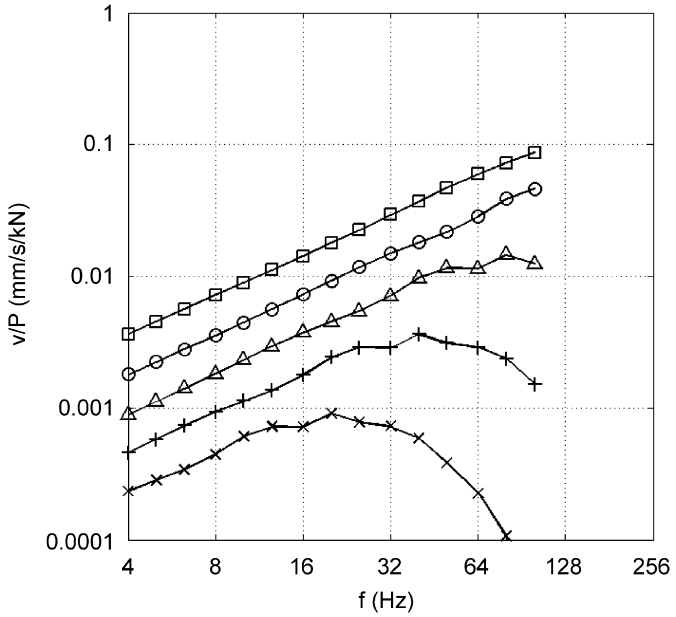


Fig. 2. Transfer function of a stiff soil with $v_S = 300$ m/s, $D = 5\%$ at the distances □ 4, ○ 8, △ 16, + 32 and × 64 m.

stationary load. The absolute maximum of the displacements is found for a number of load speeds $v_T$—for higher load speeds behind the load—and displayed in Fig. 6 as a normalized function $u/u_0(v_T/v_S)$ of the load speed. This function starts at $u/u_0 = 1$ for a stationary load and increases with increasing load speed. A maximum is reached approximately at the wave speed $v_S$ of the soil. The amplification $u/u_0$ at a super-critical speed is generally lower than at the critical speed. The maximum effect for a certain excitation frequency, for example $u/u_0 = 4$ for 8 Hz in Fig. 5, is taken to construct a general diagram (Fig. 7) for the moving-load effect

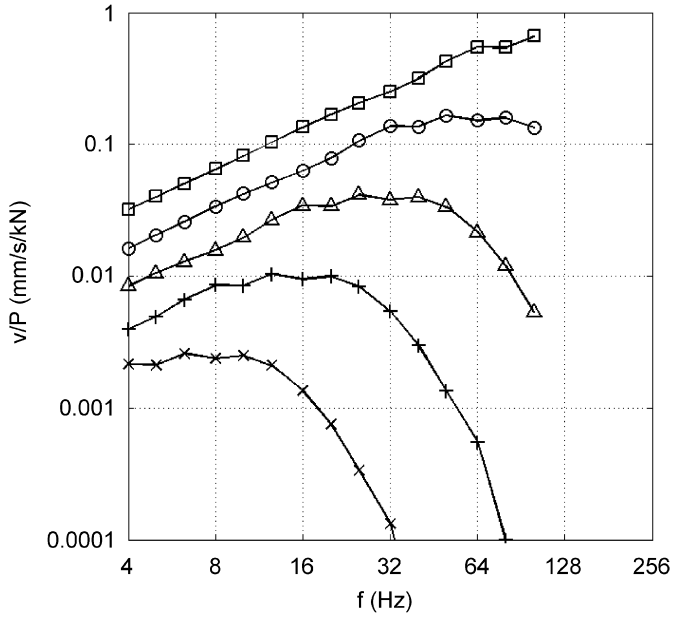


Fig. 3. Transfer function of a soft soil with $v_S = 100\,\mathrm{m/s}$, $D = 5\%$ at the distances □ 4, ○ 8, △ 16, + 32 and × 64 m.

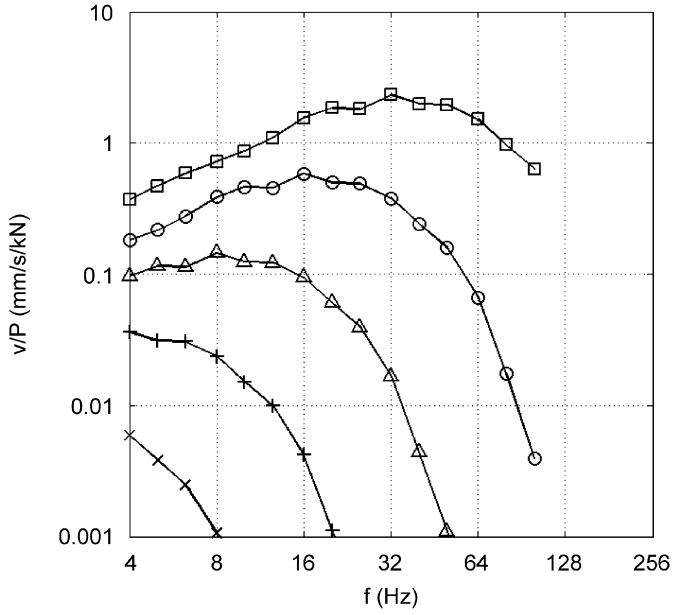


Fig. 4. Transfer function of a very soft soil with $v_S = 30\,\mathrm{m/s}$, $D = 5\%$ at the distances □ 4, ○ 8, △ 16, + 32 and × 64 m.

of harmonic loads. Fig. 7a shows considerable effects for a theoretical situation of a medium stiff soil ($v_S = 200\,\mathrm{m/s}$) and a small load area ($a = 1\,\mathrm{m}$). The maximum effect $u/u_0 = 7$ is observed at low frequencies while the effect is continuously decreasing with increasing frequency. The influence of the distance from the track ($x = 4$, 8 and 16 m) is not significant.

If the same calculations are performed for a more realistic situation with $v_S = 100\,\mathrm{m/s}$ and $a = 2.6\,\mathrm{m}$ (Fig. 7b), the influence of the load speed is much weaker and limited to a factor of 2 in the typical frequency range. To understand this different behaviour, both results are presented together in non-dimensional form in Fig. 8. The frequency is replaced by $a\,f/v_S$ and both results fit well in a single decaying curve. The parameter

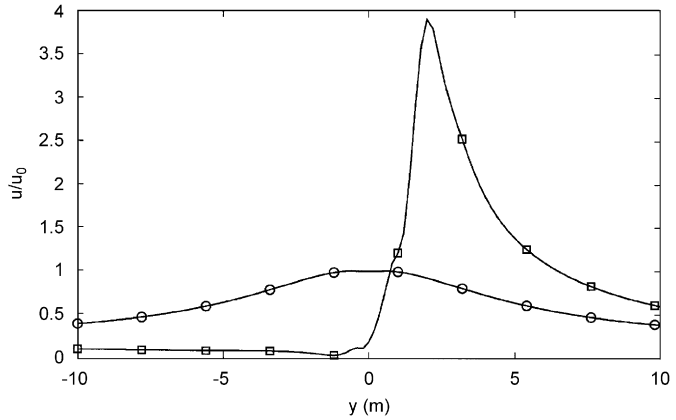


Fig. 5. Relative displacement amplitudes $u/u_0$ along the track at distance $x = 4\,\mathrm{m}$ for a harmonic square load of $a = 1\,\mathrm{m}$, $f = 8\,\mathrm{Hz}$, $v_S = 100\,\mathrm{m/s}$, □ moving load with $v_T = v_S$ and ○ stationary load.

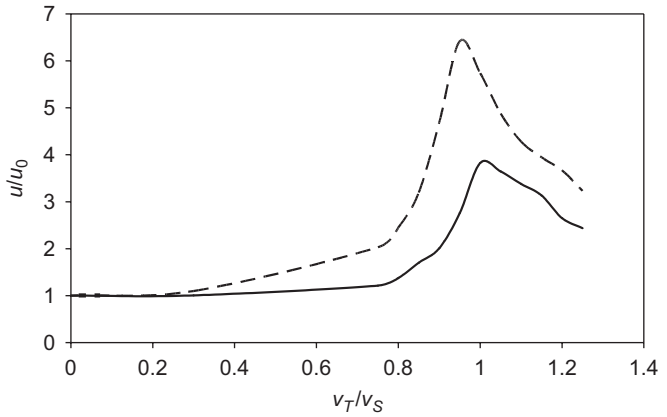


Fig. 6. Moving-load effect for a harmonic square load of $a = 2.6\,\mathrm{m}$ on a soil with $v_S = 30\,\mathrm{m/s}$, amplification $u/u_0$ of the maximum amplitude at a distance of 4 m as a function of the relative train speed $v_T/v_S$, dashed line $f = 0\,\mathrm{Hz}$ and full line $f = 1\,\mathrm{Hz}$.

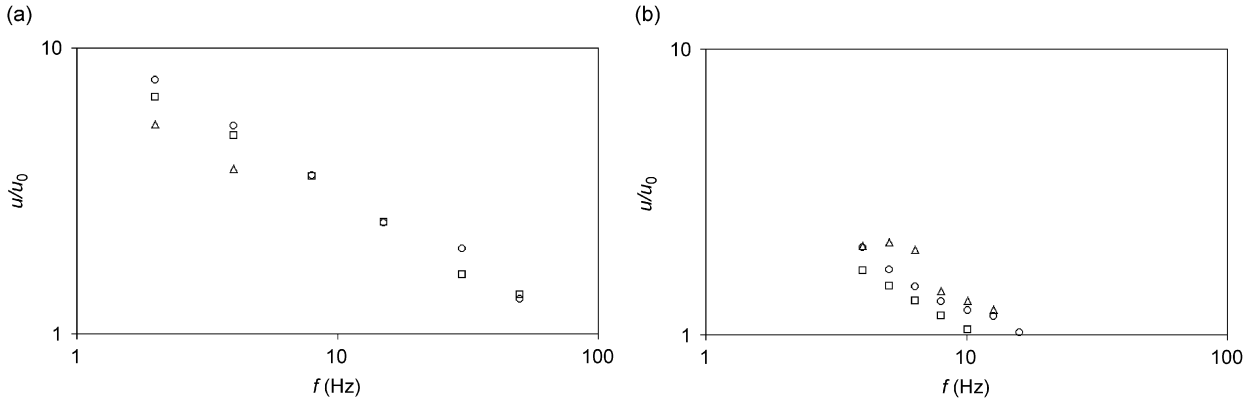


Fig. 7. Amplification $u/u_0$ of the soil vibrations at distances □ 4, ○ 8 and △ 16 m due to a harmonic load moving with critical speed $v_T = v_S$ as a function of excitation frequency: (a) for $a = 1\,\mathrm{m}$, $v_S = 200\,\mathrm{m/s}$ and (b) for $a = 2.6\,\mathrm{m}$, $v_S = 100\,\mathrm{m/s}$.

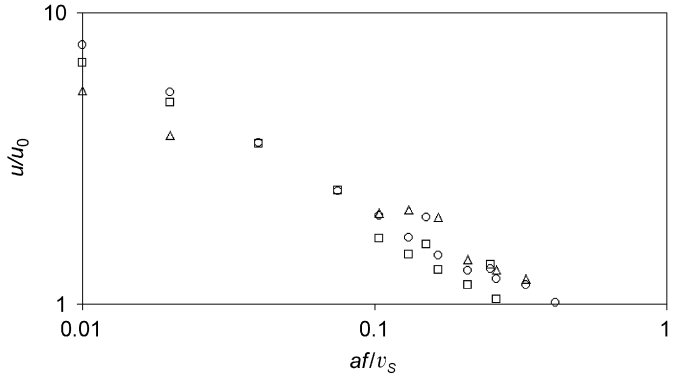


Fig. 8. Amplification $u/u_0$ of the soil vibrations at distances □ 4, ○ 8 and △ 16 m due to a harmonic load moving with critical speed $v_T = v_S$ as a function of the normalized excitation frequency $af/v_S$.

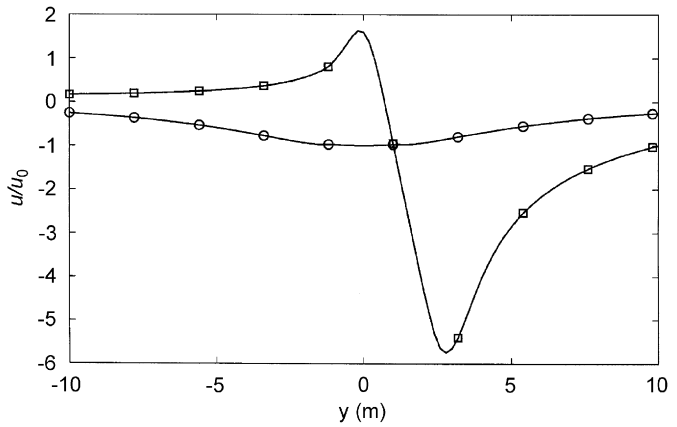


Fig. 9. Relative displacements $u/u_0$ along the track at distance $x = 4$ m for a static square load of $a = 2.6$ m, $v_S = 30$ m/s, □ moving load with $v_T = v_S$ and ○ stationary load.

$a^* = a\,f/v_S$ compares the width of the load area with the wavelength of the soil. The longer the waves are compared to the load area, the more coherent are the arriving waves of the different excitation points and the stronger is the effect at critical speed. The phase differences at a receiver point increase with higher frequencies and prevent strong effects for moving harmonic loads. The calculated effects with a maximum factor of 2 for realistic situations are almost negligible compared to the strong influence of the soil stiffness. The strongest moving-load effect may be expected for the constant static load which is examined in the following subsection.

### 3.2. The effect of moving constant loads on the soil vibration

As in the preceding subsection, the displacements on a parallel line at a distance $x$ from the track are calculated (Fig. 9). The maximum displacement, which is behind the load for the critical train speed, is evaluated and compared with the theoretical value

$$u_0 = \frac{1-\nu}{2\pi x G} P \tag{22}$$

of a stationary static load on a homogeneous half-space. The maximum amplification $u/u_0$ is calculated for different distances from the track ($x = 4$, 8, 16 m), different load areas ($a = 0.5$, 1, 2 m) and for two damping values ($D = 2.5\%$ and 5%). It can be seen from Fig. 10 that the influence of $x$ and $a$ is not so strong, especially for $D = 5\%$, whereas the influence of the damping is important for the moving constant load. Half the

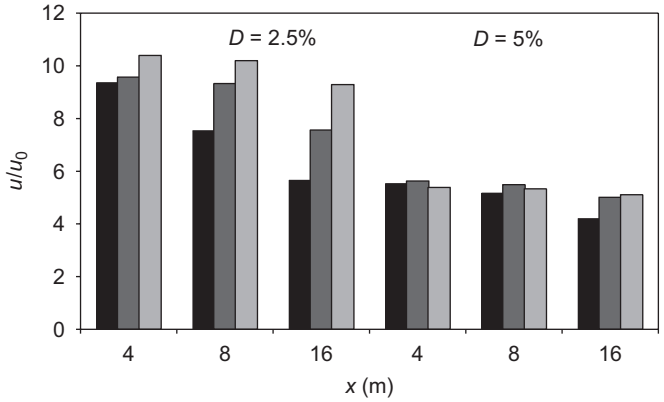


Fig. 10. Moving-load effect of constant loads on a soft soil with $v_S = 30$ m/s, amplification $u/u_0$ for different damping values $D$, different distances $x$ and different load areas, black $a = 0.5$ m, dark grey $a = 1$ m and light grey $a = 2$ m.

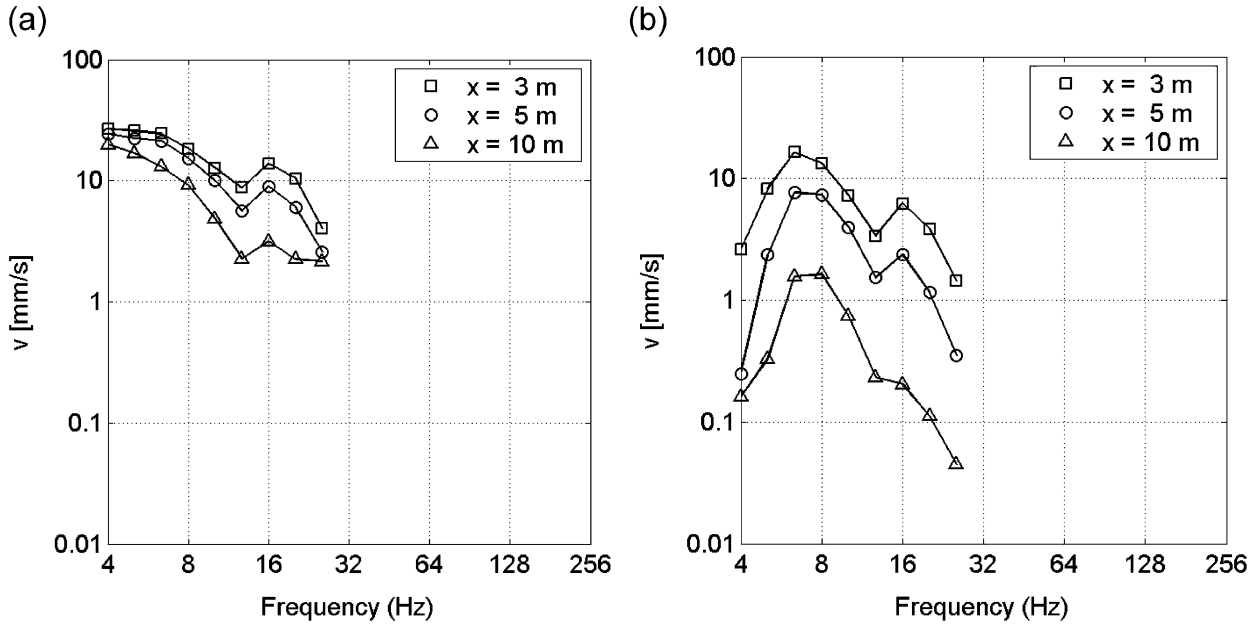


Fig. 11. Spectra of the particle velocities at distances □ 3, ○ 5 and △ 10 m due to the passage of a constant load with $P = 100$ kN and $v_T = 100$ km/h over a soft soil: (a) homogeneous soil with $v_s = 30$ m/s and (b) layered soil with $v_S = 30$ m/s over $v_S = 300$ m/s, $h = 3$ m.

damping yields almost twice the maximum amplification which reaches a value of more than 10 for a moderate damping of 2.5%.

Another strong effect due to a moving constant load can be seen in Fig. 9. The stationary load yields a smooth variation alongside the track whereas the moving load yields a sharp pulse which consists of a first upward motion and a stronger downward motion. This implies a strong change of the spectrum of the particle velocity at a fixed receiver point. The velocity spectra are calculated with different displacement solutions $u(y)$ which are transformed from the spatial domain to the time domain, from the time domain to the frequency domain and finally multiplied by $i\omega$. The strongest moving-load effect is shown in Fig. 11a where a load is moving at critical speed on a homogeneous soft soil. High amplitudes of 20–30 mm/s are calculated at the near-field which are weakly decreasing with frequency. Moreover, the attenuation of the amplitudes with distance is weak so that the response to the critically moving constant load is more important at further

distances and higher frequencies. In addition to the homogeneous soil (Fig. 11a), a layered soil, which represents the site conditions of the very soft soil, is analysed in Fig. 11b. The low-frequency beginning of the curves is much lower with amplitudes between 0.3 and 3 mm/s. Due to the layering, there is a resonance at around 6 Hz, but the resonance amplitudes are not higher than the amplitudes of the homogeneous case (Fig. 11a).

### 3.3. Soil vibration measurements on stiff and soft soils

Measured soil vibrations are compared for two sites with a normally stiff soil (site A) and a very soft soil (site B). The wave speed of the soil at the measuring site A is determined by a delay-time measurement which results in a shear wave speed of $v_S = 270$ m/s for impulse and harmonic excitation. The material damping of the soil is established from the amplitude-distance law as $D \approx 5\%$ [24,25]. Moreover, the measurements with the impulse excitation are used to evaluate the transfer function of the soil (Fig. 12). The very small amplitudes at low frequencies are due to the stiff subsoil which is assumed at 5 m depth with $v_S \approx 1000$ m/s.

Similar investigations as for the stiff soil have been performed for the very soft soil at measuring site B. The time histories of the impulse excitation are shown in Fig. 13 and the clear wave front of the dominating vibration yields a wave speed of $v = 30$ m/s. There are two minor wave fronts with higher wave velocities. The first wave front belongs to the compressional wave and the second wave front indicates a stiffer soil with $v = 300$ m/s at greater depth. An experimental transfer function of this very soft site is established (Fig. 14) where the low frequencies are dominating in clear contrast to the normally stiff soil (Fig. 12). The high frequencies are filtered by the material damping which is approximated by $D = 5\%$.

### 3.4. Measured train induced vibrations of stiff and soft soils

The train induced ground vibrations are compared for the two measuring sites which have been described in the preceding section. The velocity spectra of the measuring points at 3–50 m distance from the track are shown in Fig. 15 for the stiff and in Fig. 16 for the very soft soil. At the normally stiff site, the maximum amplitudes are found between 16 and 64 Hz whereas the low- and high-frequency amplitudes are very small. The maximum amplitudes of the very soft soil are below 8 Hz and the spectra are decreasing with increasing frequency. Due to this strong effect of damping, the high-frequency amplitudes ($f > 20$ Hz) of the soft soil are

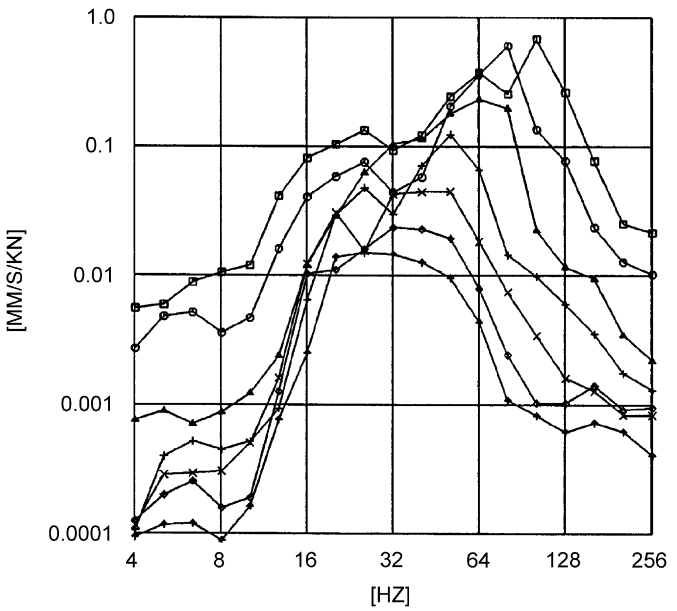


Fig. 12. Measured transfer function of the stiff soil at the distances □ 3, ○ 5, △ 10, + 15, × 20, ◇ 30 and ▽ 40 m.

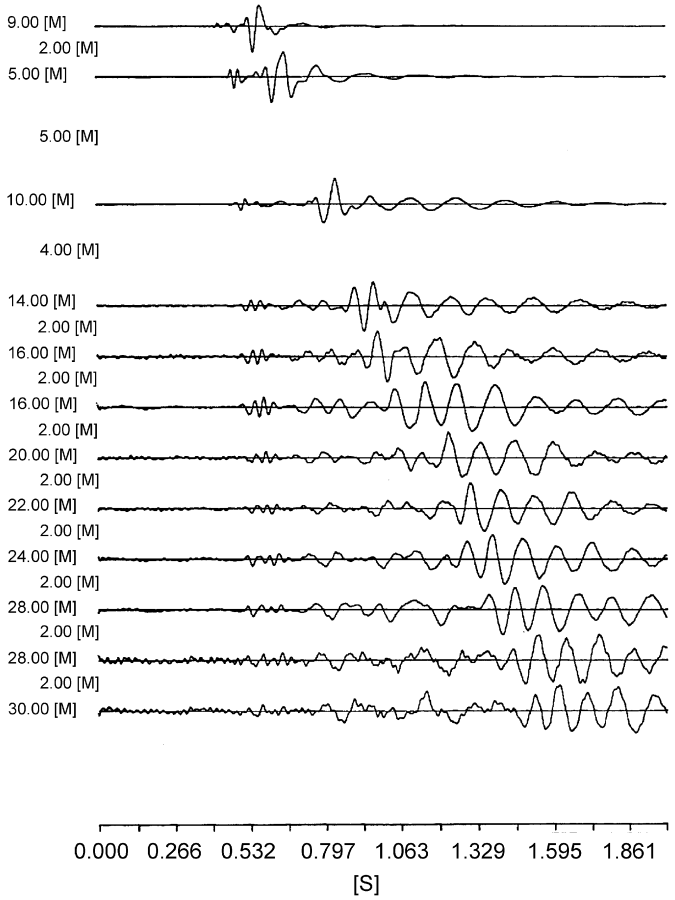


Fig. 13. Measured time histories due to an impulse excitation of the soft soil with $v_S = 30\,\mathrm{m/s}$.

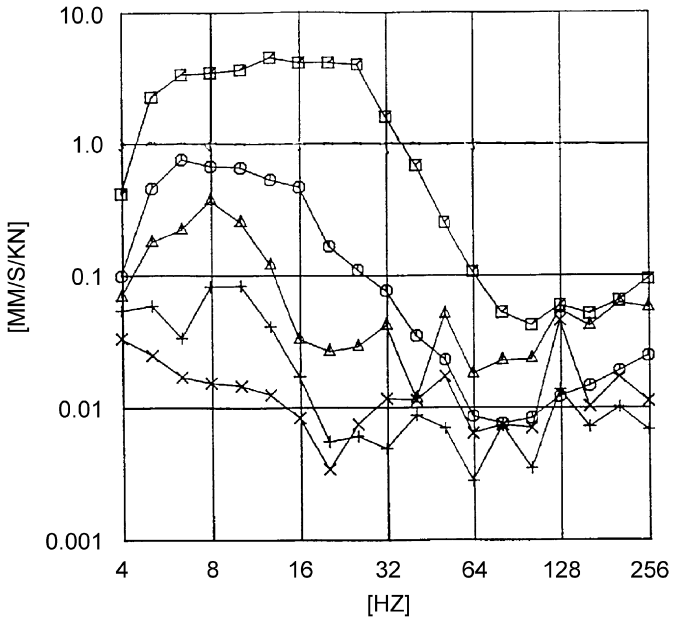


Fig. 14. Measured transfer function of the soft soil at the distances □ 3, ○ 10, △ 20, + 30 and × 50 m.

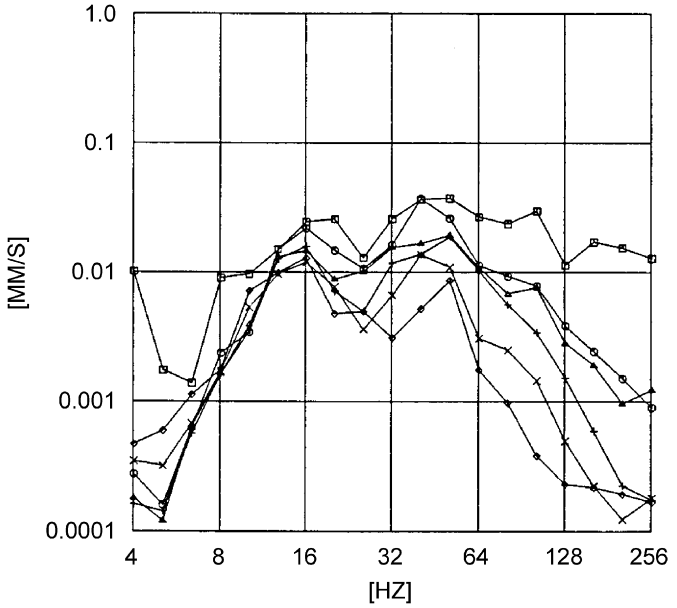


Fig. 15. Measured amplitudes of the stiff soil at $x = \square$ 3, $\circ$ 8, $\triangle$ 12, $+$ 20, $\times$ 30 and $\diamond$ 50 m during the passage of a passenger train with $v_T = 100$ km/h.

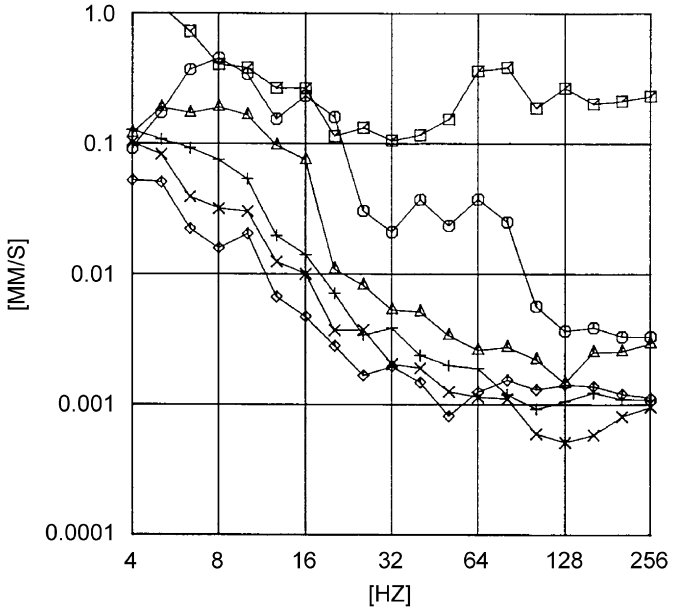


Fig. 16. Measured amplitudes of the soft soil at $x = \square$ 3, $\circ$ 10, $\triangle$ 20, $+$ 30, $\times$ 40 and $\diamond$ 50 m during the passage of a passenger train with $v_T = 100$ km/h.

smaller than those of the stiff soil. If the amplitudes of the normally stiff and the very soft soil are compared at low frequencies, a very strong difference is recognized where the amplitudes of the soft soil are about 100 times higher than the amplitudes of the stiff soil. This difference can be explained by the different shear moduli of the two sites.

If the measured amplitudes of the very soft soil (Fig. 16) are compared with the theoretically predicted amplitudes for a static axle load that is moving with critical speed on a homogeneous soil (Fig. 11a), the very

high values due to the moving-load effect cannot be found. Even the lower theoretical amplitudes of a layered soil (Fig. 11b) are not reached by the measurements. In contrary, it was shown in Ref. [21] that the measured amplitudes of the very soft soil can be predicted with a dynamic load spectrum which consists of $P_i = 1$ kN for each axle and one-third octave band and which is also suitable for a stiff soil.

The explanation for this experimental observation is as follows: The strong moving-load effect for a static load that is moving with critical speed strictly depends on the perfectly homogeneous soil conditions. The strong effect, which is due to a "sonic boom", is easily destroyed by any disturbance of the perfect soil condition. Every soil has an increasing stiffness with depth. A very soft soil normally lies on a stiffer subsoil. It is theoretically shown in Fig. 11b that this layering already reduces the moving-load effect considerably. In addition, every soil has random material properties which vary from place to place in horizontal as well as in

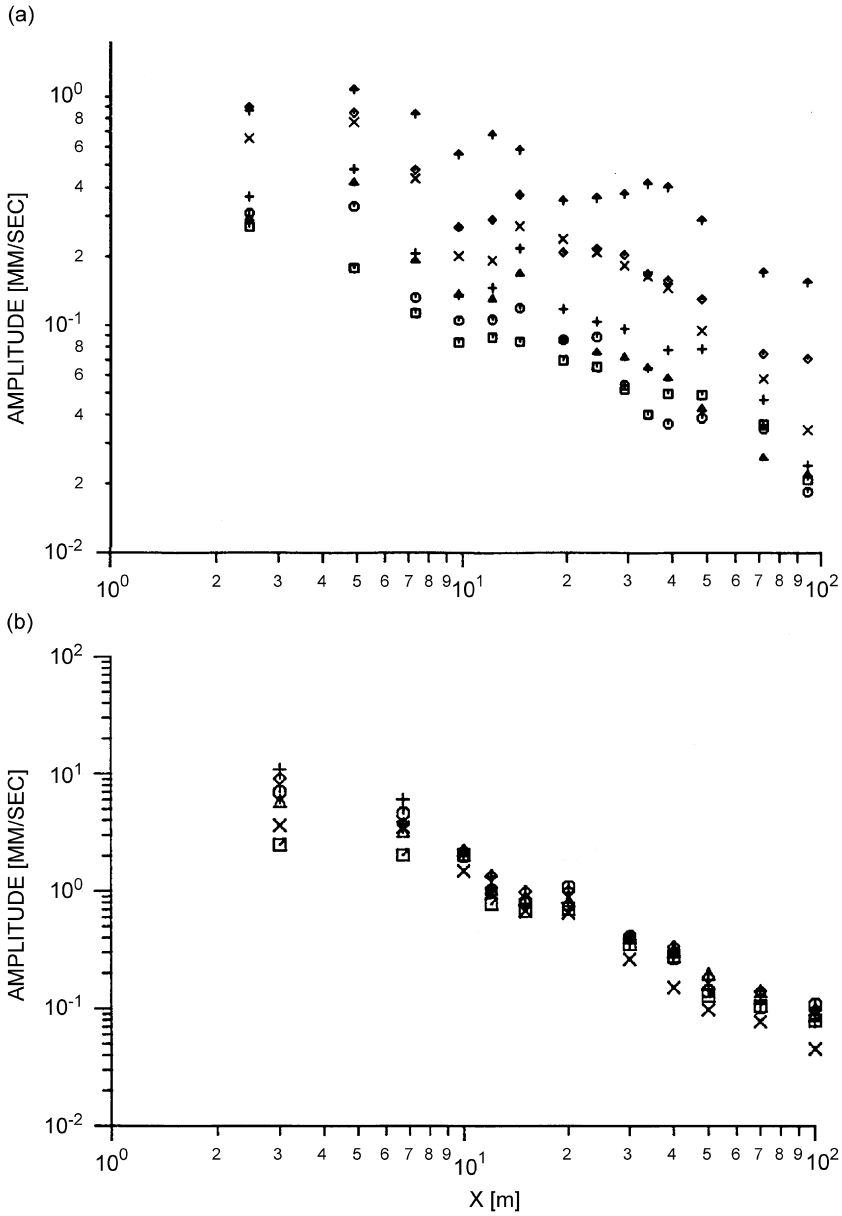


Fig. 17. Maximum amplitudes as a function of the distance due to the passages of a train with (a) $v_T =$ □ 40, ○ 60, △ 80, + 100, × 120, ◇ 140 and ▽ 160 km/h, stiff soil, and (b) different trains with $v_T = 90$–110 km/h, soft soil.

vertical direction. It is expected that this random variation of soil properties further reduces the moving-load effect in real situations.

Finally, the maximum amplitudes during the passage of trains are compared for the two sites. At the stiff site A, a measuring train with a measuring car ran on that line with different train speeds from 40 to 160 km/h [26]. The different maximum amplitudes of the corresponding speeds and all measuring points are presented in Fig. 17a. Typical values for 100 km/h, the speed considered here, are $v = 0.3$ mm/s at $x = 8$ m, $v = 0.2$ mm/s at $x = 15$ m, and $v = 0.1$ mm/s at $x = 30$ m. The attenuation of the amplitudes with distance is approximately $A \sim x^{-0.7}$ which is a typical result at railway lines. The amplitudes increase by a factor of 10 when the train speed is varied from 40 to 160 km/h, that means an increase of $A \sim v_T{}^{1.5}$.

At the soft site B, the maximum amplitudes during the passage of some trains, which are all running close to the critical speed, are plotted in Fig. 17b. The soil amplitudes reach $v = 10$ mm/s near the ballast and attenuate rather rapidly as

$$A \sim x^{-1.5}$$

due to the strong effect of material damping. At $x = 10$ m from the track, typical amplitudes are $v = 2$ mm/s, and at $x = 30$ m, amplitudes less than $v = 0.5$ mm/s are measured for all trains. Comparing the different sites, the maximum soil amplitudes at the far field have only a moderate ratio of $v_{\text{soft}}/v_{\text{stiff}} = 5$ although the stiffness ratio $G_{\text{stiff}}/G_{\text{soft}} = 100$ is very high.

## 4. Track vibrations due to critically moving trains

### 4.1. Tracks on different soils

A typical railway track is calculated as a beam on different soil models. The track beam represents the stiffness and mass of the two UIC60 rails

$$EI = 2 \times 6.4 \times 10^6\,\text{N m}^2,$$
$$m_1' = 2 \times 60\,\text{kg/m}$$

and the mass of the concrete sleepers

$$m_2' = 300\,\text{kg}/0.6\,\text{m} = 500\,\text{kg/m}.$$

The track width is

$$a = 2.6\,\text{m}$$

corresponding to the sleeper length.

The calculated displacements $u(y)$ of this track are shown in Figs. 18–20 as time histories $u(t)$ and $v(t)$ of displacement and velocity which can be compared with the measured track vibration. The results are shown for a stationary load and for a load moving with a speed of $v_T = 100$ km/h $= 28$ m/s. On the stiff soil ($v_S = 300$ m/s, Fig. 18), the maximum track displacement under a static axle load of $P = 100$ kN is

$$u_1 = 0.2\,\text{mm},$$

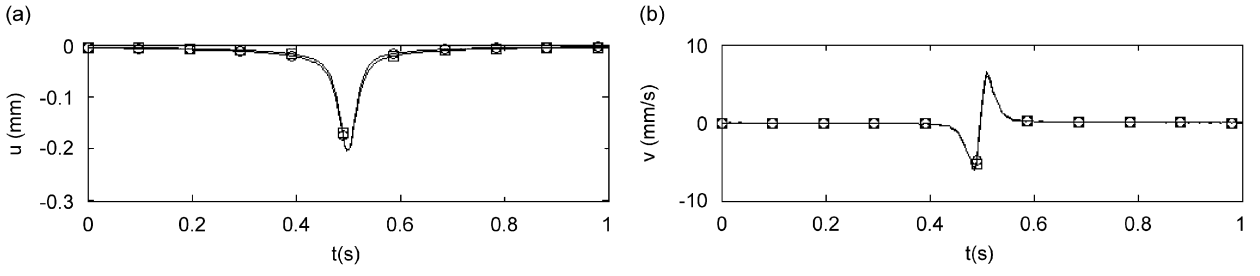


Fig. 18. (a) Displacement and (b) velocity time histories of a track on a stiff soil with $v_S = 300$ m/s during the passage of a single axle of 100 kN with train speed $v_T = 28$ m/s $\ll v_R$, calculated from the displacements $u(y)$ of □ a stationary load and ○ a moving load.

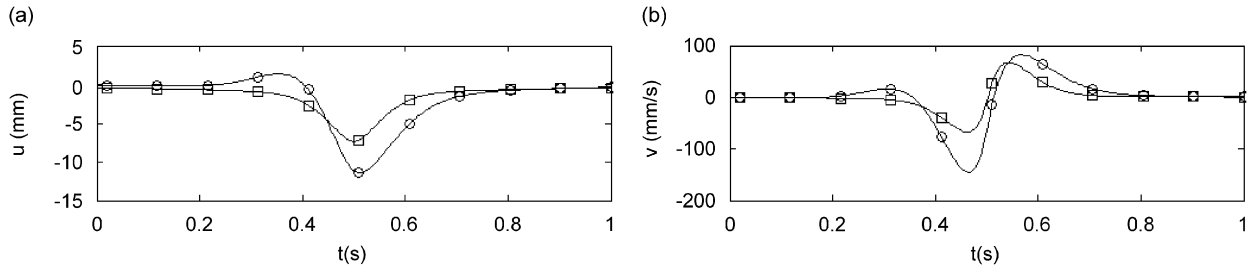


Fig. 19. (a) Displacement and (b) velocity time histories of a track on a soft soil with $v_S = 30$ m/s during the passage of a single axle of 100 kN with train speed $v_T = v_R = 28$ m/s, calculated from the displacements $u(y)$ of □ a stationary load and ○ a moving load.

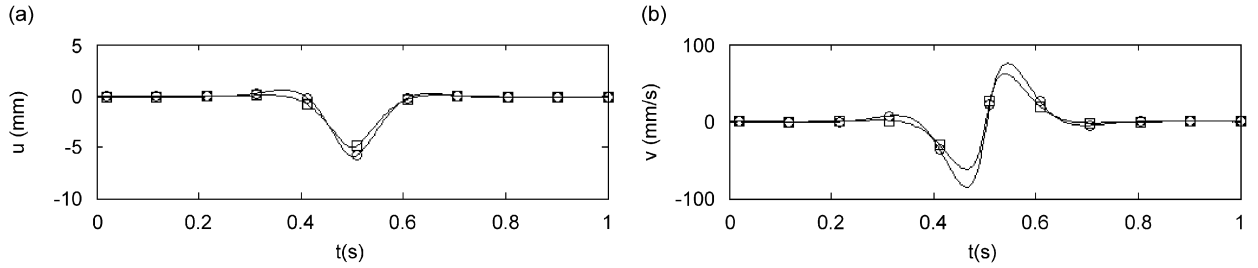


Fig. 20. (a) Displacement and (b) velocity time histories of a track on a layered soil ($v_S = 30/300$ m/s, $h = 3$ m) during the passage of a single axle of 100 kN with train speed $v_T = v_{R1} = 28$ m/s, calculated from the displacements $u(y)$ of □ a stationary load and ○ a moving load.

and the maximum velocity is

$$v_1 = 6\,\text{mm/s}.$$

The train speed is considerably slower than the Rayleigh wave velocity so that the curves of the stationary and moving load are completely identical.

If the same track is laid on the very soft soil with $v_S = 30$ m/s, it shows quite different displacements (Fig. 19). The maximum displacement is

$$u_2 = 7\,\text{mm}$$

and the deformation of the track is much wider than for the stiff soil, so that a smoother variation with distance and time is observed. The maximum track velocity is increased to

$$v_2 = 66\,\text{mm/s}$$

but the amplitude ratio between the soft and stiff soil is only $v_2/v_1 = 11$ for the velocities compared to a ratio of $u_2/u_1 = 35 \approx (G_2/G_1)^{-0.75}$ [27] for the displacement.

In addition to this strong influence of the stiffness of the soil, there is a moving-load effect for the very soft soil and the critical train speed in Fig. 19. The two curves of a stationary and a moving load differ by a moderate factor of $u/u_0 = 1.5$ for the displacement and $v/v_0 = 2.2$ for the velocity. The displacements due to the moving load show an additional small maximum before the load which is followed by a strong descent. The descent is still present at the loading point $y = 0$, and the maximum displacement is slightly a little behind the loading point. If the track is laid on a layered soil (Fig. 20), the absolute amplitudes are reduced due to the stiffer subsoil. The reduced values are 5 mm for the displacement and 60 mm/s for the velocity. The moving-load effect is also reduced for the layered situation. The amplifications compared to the stationary load are almost negligible, the values are $u/u_0 = 1.2$ for the displacement and $v/v_0 = 1.5$ for the velocity.

Track vibrations have also been measured at the same stiff and soft sites, where the soil vibrations have been measured. The track vibrations are measured by a velocity transducer (geophone) on the sleeper. The track displacements are obtained from these velocity measurements as follows (Fig. 21): The spectrum of the

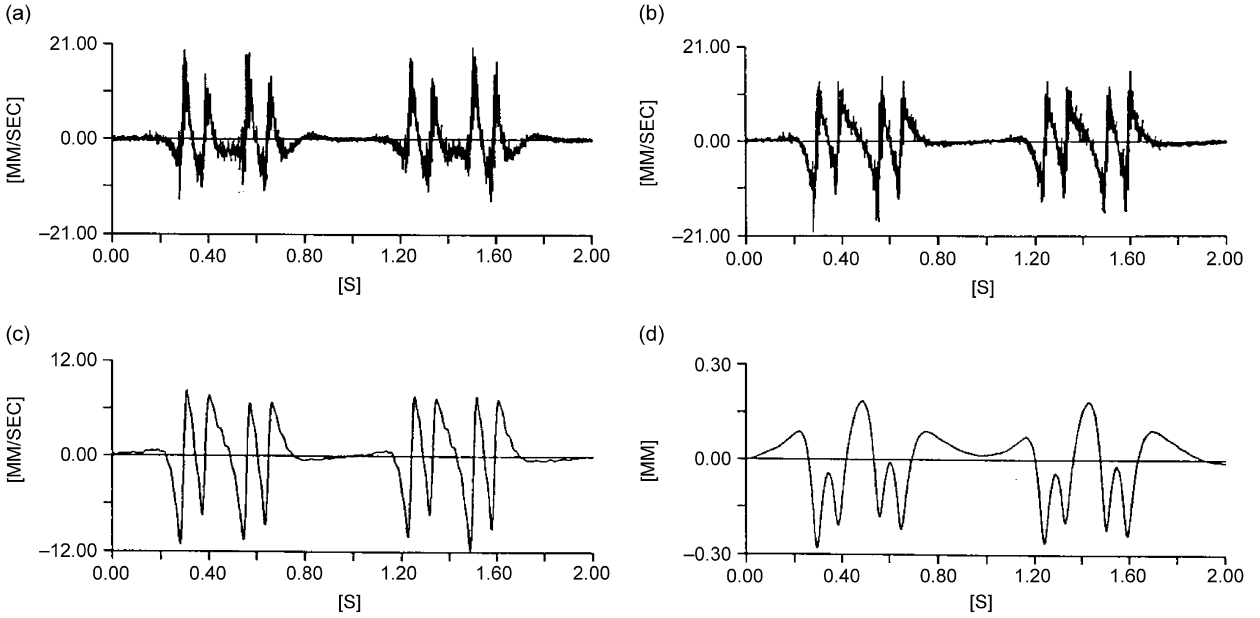


Fig. 21. Measured velocities and displacements of the track on the stiff soil during the passage of a passenger train: (a) original velocity signal, (b) corrected signal, (c) filtered signal and (d) displacements by integration of (c).

geophone is divided by the transfer function of the sensor. The inverse Fourier transform yields the corrected velocity signal (Fig. 21b). The next step is a low-pass filtering of the signal with a cut-off frequency of 30 Hz (Fig. 21c). At the end, the spectrum is divided by $i\omega$ and the inverse Fourier transform yields the displacement of the track (Fig. 21d). Fig. 21 shows the passage of four bogies of three passenger cars with a speed of 100 km/h. Every axle gives a clear impulse for the track on the stiff soil in the same way as calculated. From the given evaluation of the track measurements, approximate maximum amplitudes can be derived for the stiff soil (Fig. 21) as well as for the soft soil (Fig. 22): displacements of the stiff soil $u_1 \approx 0.2$ mm, velocity of the stiff soil $v_1 = 11$ mm/s, displacements of the soft soil $u_2 = 3$ mm, velocity of the soft soil $v_2 \approx 40$ mm/s.

Similarly to the calculated results, the measured reaction of the track on the soft soil (Fig. 22) is much smoother than on the stiff soil, so that the impulses due to following axles are not so clearly separated. Six axles from the beginning of the train passage can be identified from the original velocity signal (Fig. 22a), but not all axles are visible in the smoother displacement signal (Fig. 22d). The influence of the soil stiffness can be quantified from the measurements as $u_2/u_1 \approx 12$ for the displacements and $v_2/v_1 \approx 3.5$ for the velocities. These effects are not so strong as calculated, but still demonstrate the strong influence of the soil stiffness. In case of a soft soil, it is necessary to include the stiffening effects of the ballast, sub-ballast and the embankment. More details about track models and their verification are presented in Ref. [27].

Figs. 23 and 24 compare the spectra of the track velocity for the stiff and soft soil. The spectrum at the stiff site (Fig. 23) has a maximum between 8 and 12 Hz in case of $v_T = 100$ km/h. At higher frequencies, the amplitudes keep nearly constant at a lower level than this maximum. The track spectrum for the soft soil (Fig. 24) has the maximum of the velocity amplitudes below 4 Hz (the maximum of the theoretical results for a single axle is at 2 Hz for the soft soil and at 9 Hz for the stiff soil). Above 4 Hz, the spectrum decreases, starting with higher values ($v \leqslant 10$ mm/s) than for the stiff soil and reaching values of $v \leqslant 1$ mm/s at 16 Hz. The response to the static train loads is expected to decrease continuously with increasing frequency. Therefore, the almost constant amplitudes, that are measured at frequencies higher than 16 Hz, are due to other sources, for example irregularities of the track and vehicle [2].

### 4.2. Track on soft isolation elements

Soft isolation elements such as rail pads, sleeper shoes and ballast mats are used in tracks to reduce the dynamic loads and the vibrations due to railway traffic [28]. Heavy mass–spring system tracks consist of a high

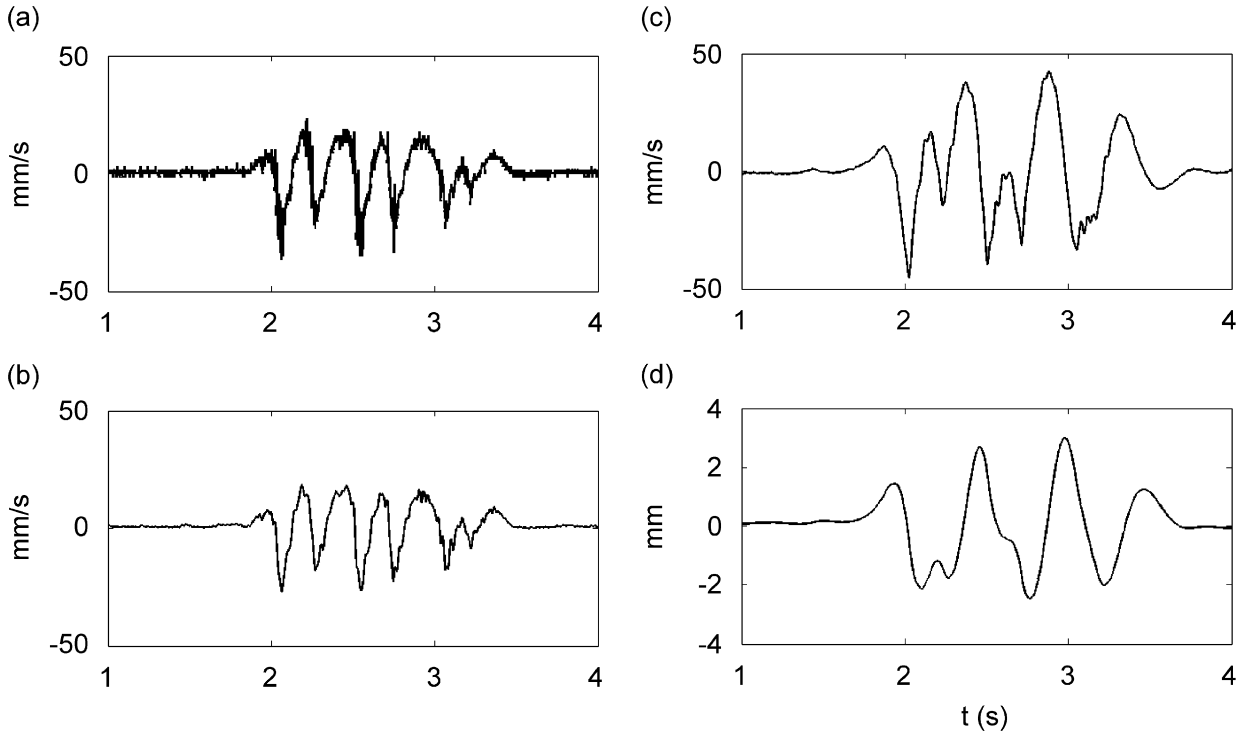


Fig. 22. Measured velocities and displacements of the track on the soft soil during the passage of a passenger train: (a) original velocity signal, (b) filtered signal, (c) corrected signal and (d) displacements by integration of (c).

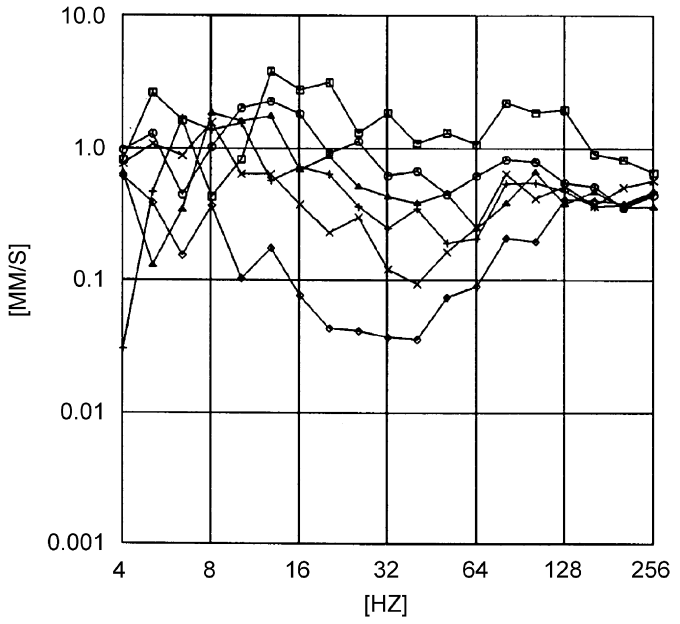


Fig. 23. Measured velocity spectra of the track on the stiff soil during the passage of passenger trains with $v_T = \square$ 160, $\circ$ 125, $\triangle$ 100, $+$ 80, $\times$ 63 and $\diamond$ 40 km/h.

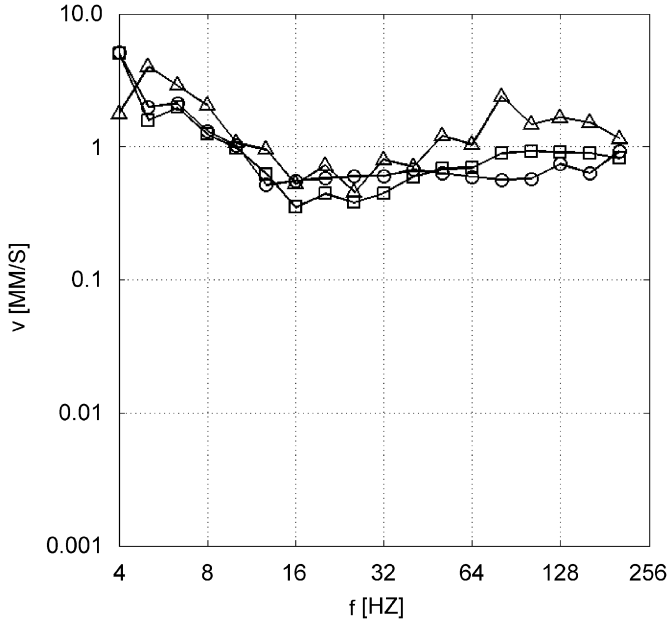


Fig. 24. Measured velocity amplitudes of the track on the soft soil during the passage of three different trains with $v_T = 100\,\mathrm{km/h}$.

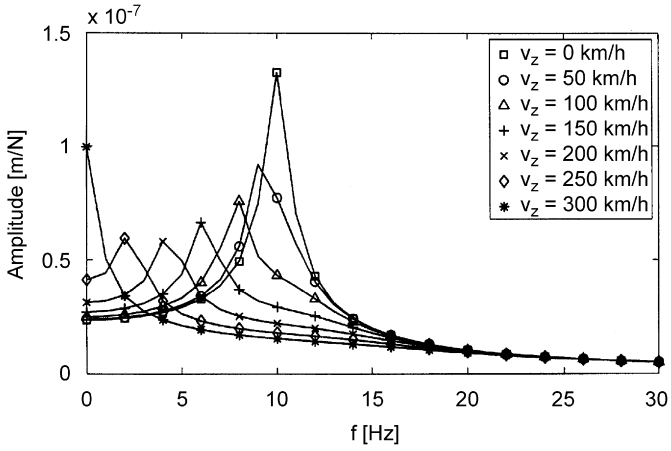


Fig. 25. Track compliance of a heavy mass–spring system under moving loads with different train speeds.

track mass due to additional concrete plates which is supported by soft springs or other elastic isolation elements. For such a heavy mass–spring system, the influence of the train speed is examined. The mass per length is chosen as $m' = 4000\,\mathrm{kg/m}$, whereas the bending stiffness is restricted to the bending stiffness of the two UIC60 rails. The stiffness of the soft isolation elements is adjusted as $k' = m'\omega_0^2$ to get the resonance frequency of $f_0 = 10\,\mathrm{Hz}$. The damping of the isolation is chosen as $D = 5\%$.

The results—the compliances of the track—are shown in Fig. 25 for different train speeds. Heavy mass–spring systems have a low resonance frequency of the track on the support which is at 10 Hz for the chosen parameters. It is observed that the resonance is shifted to lower frequencies if the speed of the train is increased. Moreover, the resonance amplitude is also reduced with increasing speed. These effects can be interpreted as if the moving load would increase the mass and damping of the track system. At $v_T = 300\,\mathrm{km/h}$, the resonance frequency is shifted to $f = 0\,\mathrm{Hz}$ and that means that the critical speed of this track system is

reached. It is the critical speed according to

$$v_{\text{critical}} = \sqrt{2\frac{\sqrt{k'EI}}{m'}} \tag{23}$$

which is different from the critical speed of the soil. The resonance amplification at this critical speed is not higher than for a stationary load. The importance of this situation is due to the fact that the high regular static train loads are amplified at the resonance instead of small irregular dynamic loads.

The calculated results are valid for the extreme situation in which the heavy mass–spring system has no bending stiffness, for example if it consists of short plate segments. If the mass–spring system is constructed as a continuous plate, the bending stiffness of the plate shifts the critical speed to very high and not accessible train speeds. In general, this type of critical train speed is found in reality less probably than a critical wave speed of the soil.

## 5. Conclusions

The effects of loads moving on the soil with critical speed are analysed by integration techniques in the frequency–wavenumber domain. The integrals for the soil and track vibrations are evaluated numerically and a parametric study of the moving-load effect is performed. Theoretical and experimental results regarding displacement and velocity amplitudes of soil and track vibrations are shown for a regular (stiff) and a very soft soil.

The parameters of the stiff soil ($v_S = 300\,\text{m/s}$, $D = 5\%$) and of the very soft soil ($v_S = 30\,\text{m/s}$, $D = 5\%$) correspond to those measured at test sites in Germany. The low-frequency amplitudes of the soft soil are 100 times higher than those of the stiff soil, and the track displacements on the soft soil are 35 times higher than those on the stiff soil. This strong influence of the soil stiffness is compared with the influence of the load speed. For moving harmonic loads, the maximum amplification at near-critical speeds depends clearly on the load frequency $f$, the load distribution across the track width $a$, and the wave velocity $v_S$ of the soil. The moving-load effect decreases with increasing parameter $af/v_S$. Therefore, the amplification of harmonic loads is limited to $u/u_0 \ll 2$ for realistic parameters. The strongest effect is found for the moving constant load for which the maximum values are $u/u_0 \approx 5$ for a soil damping of $D = 5\%$ and $u/u_0 \approx 10$ for $D = 2.5\%$. In addition to the strong amplification of the soil vibration, a small amplification $u/u_0 = 1.5$ of the track displacement under a critically moving load has been calculated. The weak or strong moving-load effects are reduced by stiffer soil layers at greater depths and by random inhomogeneities of the soil.

The results are compared with measurements at a soft and stiff site. The strong difference between the low-frequency amplitudes of the soft and stiff sites is verified by the measurements as well as the strong difference between the frequency contents—a low-frequency content in the soft soil, a high-frequency content in the stiff soil. If the maximum amplitudes are compared, there is only a moderate ratio of $v_{\text{soft}}/v_{\text{stiff}} = 5$ at the far field, although the stiffness ratio is $G_{\text{stiff}}/G_{\text{soft}} = 100$ and the train is running with the critical speed. This result can be explained by the damping and the inhomogeneity of the soil. The practical conclusion is that great care should be taken if strong moving-load effects are theoretically predicted for real situations, and that the most important parameters, the stiffness and damping of the soil, must be measured and introduced properly into the calculation.

## References

[1] X. Sheng, C. Jones, D. Thompson, Comparison of a theoretical model for quasi-statically and dynamically induced environmental vibration from trains with measurements, *Journal of Sound and Vibration* 267 (2003) 621–635.

[2] L. Auersch, The excitation of ground vibration by rail traffic, Theory of vehicle–track–soil interaction and measurements on high-speed lines, *Journal of Sound and Vibration* 284 (2005) 103–132.

[3] D. Aubry, D. Clouteau, G. Bonnet, Modelling of wave propagation due to fixed or mobile dynamic sources, *Proceedings of Wave Propagation and Reduction of Vibrations*, Berg-Verlag, Bochum, 1994, pp. 109–121.

[4] H.A. Dietermann, A.V. Metrikine, The equivalent stiffness of a half-space interacting with a beam. Critical velocities of a load moving along a beam, *European Journal of Mechanics A/Solids* 15 (1996) 67–90.

[5] H. Grundmann, M. Lieb, E. Trommer, The response of a layered half-space to traffic loads moving along its surface, *Archive of Applied Mechanics* 69 (1999) 55–67.
[6] X. Sheng, C.J.C. Jones, M. Petyt, Ground vibration generated by a load moving along a railway track, *Journal of Sound and Vibration* 228 (1999) 129–156.
[7] C. Madshus, A. Kaynia, High speed railway lines on soft ground, dynamic behaviour at critical speed, *Journal of Sound and Vibration* 231 (2000) 689–701.
[8] H. Takemiya, Simulation of track–ground vibrations due to highspeed train, *Journal of Sound and Vibration* 261 (2003) 503–526.
[9] A. Karlström, A. Boström, An analytical model for train-induced ground vibrations from railways, *Journal of Sound and Vibration* 292 (2006) 221–241.
[10] G. Lombaert, G. Degrande, J. Kogut, S. Francois, The experimental validation of a numerical model for the prediction of railway induced vibrations, *Journal of Sound and Vibration* 297 (2006) 512–535.
[11] L. Auersch, Ground vibration due to railway traffic—The calculation of the effects of moving static loads and their experimental verification, *Journal of Sound and Vibration* 293 (2006) 599–610.
[12] L. Fryba, *Vibrations of Structures under Moving Loads*, Noordhof Int. Publishing, Groningen, 1972.
[13] K. Knothe, S. Grassie, Modelling of railway track and vehicle/track interaction at high frequencies, *Vehicle System Dynamics* 22 (1993) 209–262.
[14] G. Lefeuve-Mesgouez, Propagation d'ondes dans un massif soumis à des charges se déplaçant à une vitesse constante, Thèse de Doctorat, Ecole Centrale Nantes, 1999.
[15] T. Ekevid, On computational wave propagation in solids—with emphasis on high-speed train related ground vibrations, Licentiate Thesis, CTH Göteborg, 2000.
[16] V. Krylov, Generation of ground vibration boom by high-speed trains, in: V. Krylov (Ed.), *Noise and Vibration from High-Speed Trains*, Telford, London, 2001, pp. 251–283.
[17] G. Pflanz, Numerische Untersuchung der elastischen Wellenausbreitung infolge bewegter Lasten mittels der Randelementmethode im Zeitbereich, Dissertation, Universität Bochum, 2001.
[18] L. Andersen, S. Nielsen, S. Krenk, Numerical methods for analysis of structure and ground vibration from moving loads, *Computers and Structures* 85 (2007) 43–58.
[19] P. Bengtsson, et al., High speed lines on soft ground—measurements from the west coast line at Ledsgard. Banverket Report, Borlänge, Sweden, 1999.
[20] K. Adolfsson, B. Andreasson, P. Bengtsson, P. Zackrisson, Highspeed train X2000 on soft organic clay—measurements in Sweden, *Proceedings of the 12th European Conference. Soil Mechanics and Geotechnical Engineering*, Balkema, Rotterdam, 1999, pp. 1713–1718.
[21] L. Auersch, Wave propagation in layered soil, theoretical solution in wavenumber domain and experimental results of hammer and railway traffic excitation, *Journal of Sound and Vibration* 173 (1994) 233–264.
[22] J. Wolf, *Dynamic Soil-Structure Interaction*, Prentice-Hall, Englewood Cliffs, NJ, 1985.
[23] M. Steenbergen, A. Metrikine, The effect of the interface conditions on the dynamic response of a beam on a half-space to a moving load, *European Journal of Mechanics A/Solids* 26 (2007) 33–54.
[24] L. Auersch, Zur Entstehung und Ausbreitung von Schienenverkehrserschütterungen, Theoretische Untersuchungen und Messungen am Hochgeschwindigkeitszug Intercity Experimental, BAM-Forschungsbericht 155, Berlin, 1988.
[25] L. Auersch, Parametric excitation of rail-wheel-system, calculation of vehicle-track-subsoil-dynamics and experimental results of the high speed train Intercity Experimental, *Archive of Applied Mechanics* 60 (1990) 141–156.
[26] L. Auersch, S. Said, W. Rücker, Das Fahrzeug-Fahrweg-Verhalten und die Umgebungserschütterungen bei Eisenbahnen. BAM-Forschungsbericht 243, Berlin, 2001.
[27] L. Auersch, Dynamics of the railway track and the underlying soil, the boundary-element solution, theoretical results and their experimental verification, *Vehicle System Dynamics* 43 (2005) 671–695.
[28] L. Auersch, 2- and 3-dimensional methods for the assessment of ballast mats, ballast plates and other isolators of railway vibration, *International Journal of Acoustic and Vibration* 11 (2006) 167–176.